PROTOTYPE OF INNOVATIVE WHEEL DIRECT DRIVE WITH WATER-COOLED AXIAL-FLUX PM MOTOR FOR ELECTRIC VEHICLE APPLICATIONS

F. Caricchi (*), F. Crescimbini (*), A. Di Napoli (**)

(*) *University of Rome "La Sapienza"*
Department of Electrical Engineering
Via Eudossiana, 18 - 00184 Rome (Italy)

(**) *III University of Rome*
Dept. of Mechanical Eng. and Automatics
Via Segre, 8 - 00146 Rome (Italy)

Abstract - **This paper presents an innovative wheel direct drive which uses a novel topology of axial-flux permanent magnet machine having multi-stage structure and water-cooled air-wound stator winding. Battery supply of the motor is accomplished by means of a water-cooled IGBT power electronic interface which is the cascade of a bidirectional dc-to-dc buck-boost converter and current regulated PWM inverter. The paper discusses design and construction of a 25 kW prototype of the proposed wheel direct drive, which will find application in the propulsion system of a novel city car[1].**

1. INTRODUCTION

The electric vehicles of the future are expected to be propelled by direct drive wheel motors for a more efficient powertrain. In fact, by integrating the motor into the wheel, one can eliminate the need for shafts, transaxles, differentials, clutches and reduction gears, thereby eliminating transmission losses, reducing the weight of the vehicle and also simplifying greatly the mechanical design of the all electric vehicle. However, low-speed high-torque motor drives devoted to the electric vehicle application must meet tight requirements such as very high torque density and overload capability, and these severely constrain the design of both motor and power electronic circuits. Further to that, mounting the motor within the wheel is desirable but imposes a restriction on the machine diameter and demands totally-enclosed construction to provide protection against the environment. Hence, a very effective cooling of the machine is needed to achieve the all required performance.

Whilst conventional either ac excited or brushed dc motors have poor torque density and overload capability to be used as wheel direct drive motors, on the other hand, brushless dc motor drives designed for low-speed high-torque operation are drawing considerable attention for the electric vehicle application. This is mainly due to the availability of new high-energy permanent magnets, which has opened up the possibility of developing novel motor topologies with high torque-to-weight ratio and overload capability for the use in wheel direct drive.

Among a number of brushless dc motors with innovative topology being investigated, axial-flux permanent magnet machines (AFPMs) with either slotless or air-wound winding prove to be one best candidate for application in the electric vehicle, as their disc shape is well suited to the direct coupling with a wheel, and they can be designed for very high torque-to-weight ratio without loss of efficiency. AFPMs retain all the advantages inherent to conventional brushless PM motors, and in addition they offer improvements in torque ripple, reduced iron losses, more efficient heat removal from the stator winding, and simple manufacturing. In the last few years, AFPMs have been proposed for a number of motoring applications, and recently a 2.5 kW prototype of wheel direct drive with slotless axial-flux permanent magnet motor has been utilised for the propulsion of an electric scooter [1].

This paper presents a novel wheel direct drive arrangement which uses an axial-flux PM motor having multi-stage structure and water-cooled air-wound stator winding. Battery supply of the motor is accomplished by a water-cooled IGBT power electronic interface which is the cascade of a bidirectional dc-to-dc buck-boost converter and CRPWM inverter. The paper discusses design and construction of a 25 kW prototype of the proposed wheel direct drive, which will find application in the propulsion system of a novel city car being jointly developed with one major car manufacturer.

2. WHEEL DIRECT DRIVE TOPOLOGY

Fig. 1 shows the layout of the proposed wheel direct drive. It compounds a water-cooled two-stage axial-flux PM motor and a battery-fed power electronic interface which is the cascade of a bidirectional dc-to-dc converter, current-

[1]This project is supported by the CNR-PFT2

0-7803-3044-7/96 $5.00 © 1996 IEEE

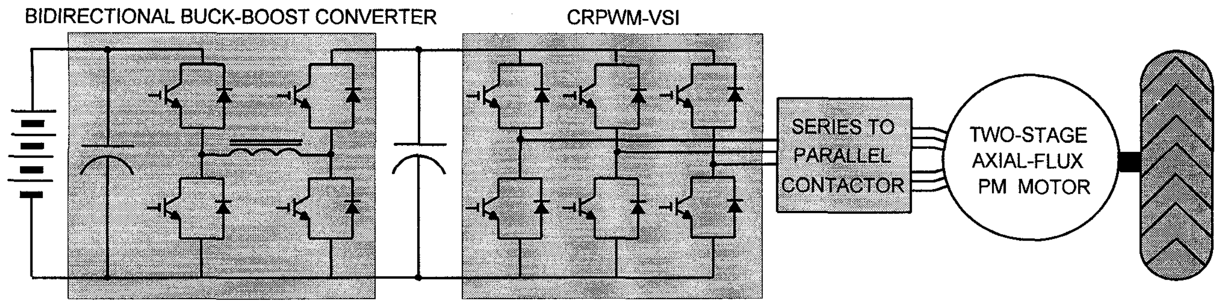

Fig. 1 Wheel direct drive with water-cooled two-stage axial-flux PM motor.

regulated PWM inverter and series-to-parallel contactor. For the purpose of rotor position sensing, an optical encoder is integrated into the motor. A description of the components of the wheel direct drive is given in the following.

A. *Water-Cooled Axial-Flux PM Motor*

In AFPMs, the electromagnetic torque is mainly a function of the machine outer diameter. If the available space is too small a diameter, then the torque required at the machine shaft can be achieved by means of a multi-stage arrangement of the machine, as shown in Fig. 2 for a two-stage machine. In a multi-stage AFPM, if j is the number of stages, then the machine has j stator windings and $(j+1)$ PM disc rotors. The $(j+1)$ rotors share a common mechanical shaft, whereas the terminals of the j three-phase windings may be connected either in series or parallel. If the connection among the machine stages is to be modified during variable-speed operation, then an inverter with reduced kVA rating can be used, as discussed later on.

AFPMs with multi-stage structure may have either iron-cored or air-wound windings. However, for the high overload capability and totally-enclosed construction required in the wheel direct drive application water-cooling of the machine is needed, and this is best accomplished with air-wound windings. Thus, the axial-flux machine arrangement shown in Fig. 2 has two air-wound stator windings which consist of coils placed side by side in a toroidal fashion and supported by a fibre-reinforced epoxy structure. Space is left between the two active sides of each coil for a duct which is used to remove heat directly from the interior surface of the winding by cooling water passing between the coil sides.

Because of the lack of the toroidal core, in a multi-stage AFPM with air-wound windings the flux driven by magnets passes axially from a north-pole on one rotor to a facing south-pole on the other, as shown in Fig. 2. The coils of the stator windings lie on the transverse plane normal to axis. Thus, the flux driven by the magnets interacts with the current commanded in the active sides of the coils to produce torque. As a result of the flux path, only the external rotor discs must be made of material with good magnetic properties (typically mild steel). The intermediate, on the other hand, is used merely for mechanical support of the magnets, and so light weight non-magnetic materials can be used for its construction thus enhancing the compactness and lightness of the machine.

The machine winding is accomplished with coils having the rhomboidal shape, since this is a coil shape which has reduced length of the end-windings due to the inclined arrangement of the coil active sides. It was shown in [2] that

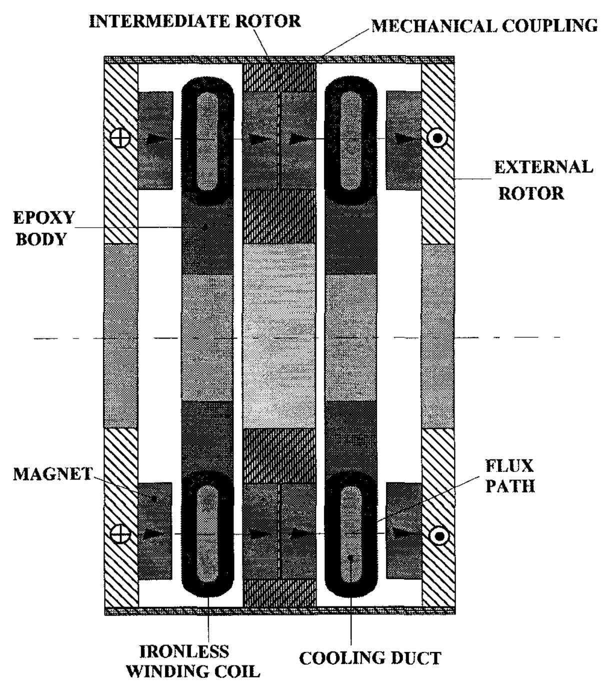

Fig. 2 Cross-section of two-stage axial-flux PM machine with water-cooled air-wound windings.

a machine winding which uses coils having the rhomboidal shape allows the achievement of much higher values of the torque per unit of I^2R, if compared with the conventional arrangement of the machine winding with coils having the trapezoidal shape.

The cooling system of the machine is shown in Fig. 3. The two hydraulic circuits of the machine stages are connected in parallel and share a common air-to-water heat exchanger. This is designed to keep the temperature of the inlet water below a desired temperature whilst dissipating the heat due to 100% overload operation of the machine. The power loss within the winding is removed by assisted circulation of cooling water with water flow of few litres per minute. This results in a relatively low overtemperature between the inlet and the outlet of the cooling duct.

The distribution of temperature around the winding follows the temperature gradient of the water along the cooling duct, but there is an overtemperature of the winding with respect to the cooling water because of the insulating enamel which coats the winding conductors. The machine winding has a hot spot the outlet of the cooling duct. For a given hydraulic radius (i.e. the thickness of the water duct), proper selection of the water flow allows overloads along several minutes running with rise of temperature in the machine winding which keeps well below the limits allowed for the class F insulating materials used.

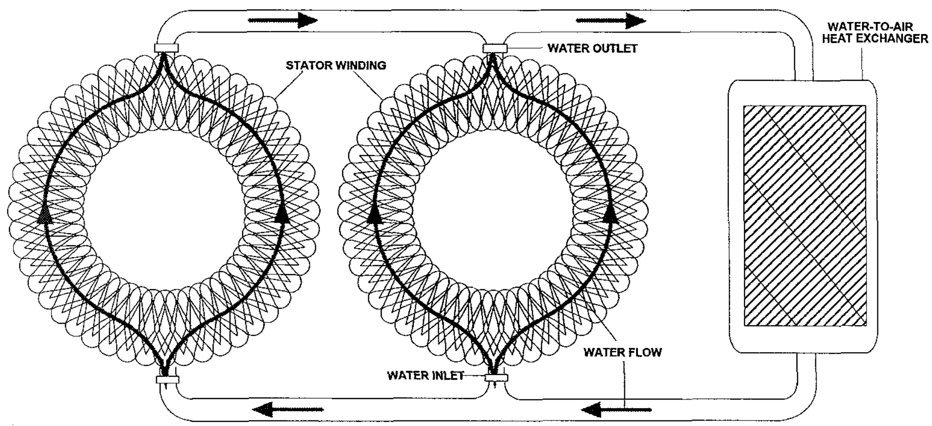

Fig. 3 Layout of the cooling system for a two-stage machine

B. Battery-Fed Power Electronic Interface

For motoring operation AFPMs require to be fed by the variable-frequency voltage supply available from a current-regulated voltage source inverter, as shown in Fig. 1. Speed variation is accomplished at open loop by the adjustment of the commanded torque. This in turn is divided by the torque constant to yield the peak value of the current that should flow in the motor phases, with just a current limit to ensure that the motor current is held within the motor's capabilities. Then, the commanded peak current is used together with the information on rotor position to generate the reference current waveforms that, from the comparison with the actual current waveforms, determine the PWM signals driving the inverter switches.

AFPMs have excellent performance for constant-torque operation, but they do not lend themselves to constant-power operation because of the particularly low value of inductance which requires a large amount of current to offset the magnet flux with stator reaction flux. Thus, variable-speed operation beyond the speed at which the line-to-line motor EMF gets near the inverter dc input voltage (i.e. the base speed of the motor) are generally not allowed since the maximum current which the inverter can deliver is fixed.

However, for given kVA rating of the inverter, the multi-stage arrangement of the machine allows to extend variable-speed operation over the base speed by switching from series to parallel the connection among the machine stages. Then, machine speeds up to the base speed are achieved with the connection in series of the machine stages, so that the maximum current which the inverter can deliver is used to produce the rated torque of the machine. When the line-to-line motor EMF gets near the inverter dc input voltage the connection between the machine stages is switched from series to parallel by means of the series-to-parallel contactor shown in Fig. 1. As the voltage at the motor terminals suddenly reduces to a half, the dc voltage available at the inverter input can still be used to deliver the maximum current of the inverter and produce half the machine rating torque for machine speeds up to twice the base speed.

The described technique is suitable for use in electric vehicles with direct-drive wheel motors, since in such a motor application the rating torque of the machine is only required at low speeds, whereas a reduced torque is generally needed at the maximum speed of the vehicle. Switching the connection between the machine stages during variable-speed operation allows a reduction in the cost of the motor drive, since an inverter with kVA rating equal to the rating power of only one stage of the machine can be used. For a two-stage machine the resulting torque vs. speed characteristic is a combination of two constant-torque regions, and this is very near the mechanical characteristic achieved at the wheel shaft of a conventional vehicle with a two-gears drive train powered by a thermal engine.

One further problem related to the low value of the machine inductance is that in axial-flux PM motor drives the waveform of the stator current may be affected by a significant ripple which produces additional I^2R losses in the winding. The magnitude of such a current ripple depends on the inverter switching frequency, but on an instantaneous basis it is also determined by the difference between the inverter input voltage and the motor EMF. Whilst the use of an inverter switching frequency as high as possible would be desirable to reduce the ripple amplitude, on the other hand, this leads to an increase of the inverter power loss.

As an alternative solution, the reduction of the motor current ripple can be achieved by adjusting continuously the inverter input dc voltage with respect to the machine EMF. To this end, a buck-boost dc-to-dc converter is used in the dc link as shown in Fig. 1, so that the inverter input voltage can be adjusted accordingly with the motor speed. Modes of operation of the dc-to-dc converter topology shown in Fig. 1 were discussed in [3] together with experimental results taken from a laboratory prototype.

The buck-boost converter used in the dc link of the proposed motor drive has a bidirectional arrangement to allow the reversal of the power flow and recovery of the vehicle kinetic energy in the battery by means of the regenerative braking operation. To achieve maximum extraction of the kinetic energy from the machine, the braking current flowing in a given phase of the motor must be in phase with the related motor EMF. This is easily accomplished with only the flywheel diodes of the PWM inverter being conducting (i.e. the all switches of the inverter bridge are kept in the off state), while the amplitude of the braking current is regulated at the desired value by the switching operation of the buck-boost converter in the dc link.

3. PROTOTYPE OF WHEEL DIRECT DRIVE

A 25 kW prototype of the wheel direct drive shown in Fig. 1 has been designed for application in the propulsion system of a newly-conceived city car. Construction of the prototype drive components has been recently completed and laboratory tests are being carried out to evaluate characteristics of the drive operation. Thereafter, a second identical drive will be constructed to complete the electric propulsion system of the vehicle for a road test programme.

The city car prototype being under development has the design characteristics given in Table I and uses a dual-power propulsion system. This means that a conventional 1000 cm^3 thermal engine is used to drive the front wheels of the vehicle, whereas the electric propulsion system with twin wheel direct drives propels the vehicle rear wheels. Either the thermal engine or electric propeller is to be operated, depending on whether the car is used for long-distance extraurban missions or moves within city areas restricted bylaw to zero-emission vehicles, respectively.

No direct connection does exist between the thermal and electric propellers, but, if needed, during thermal engine driving of the vehicle the driver may decide to temporarily operate the electric machines coupled to the rear wheels as generators, so that the battery storage can be recharged via the inverter flywheel diodes and the buck-boost dc-to-dc converter. Because of the dual-power propulsion system, the prototype vehicle is to be equipped with a battery storage of reduced size, and it was selected a set of lead-acid cells with 36 Ah capacity and rating voltage of 288 V.

Table I Design characteristics of the city car prototype.

Weight of the vehicle (including battery storage and payload)	1300	kg
Maximum speed	110	km/h
Time interval for vehicle acceleration on flat road from standstill to 100 km/h	14	s
Maximum slope climbing (@ 30 km/h)	24%	
Radius of the wheel tire under load	0.265	mm

Design of the prototype drive is based on the required vehicle performance given in Table I. It is found that the maximum gross tractive effort is needed for the vehicle climbing a 24% slope, and this results in overall torque of 860 Nm at the axles of the vehicle wheels. Hence, the required maximum torque can be achieved with 100%

overload of two twin wheel motors, being each motor rated 215 Nm, 1100 rpm.

A. *Prototype of Wheel Motor*

As mentioned in a preceding section of this paper, the torque T developed at the motor shaft is a function of the machine outer diameter, and it can be written as:

$$T = k \cdot R^3 \quad (1)$$

where R is the outer radius of the machine and k is a design constant which has a value in the range from 25000 to 30000 Nm/m^3, depending on a number of machine design variables. Hence, from (1) it is found that a single-stage machine gives the required torque of 215 Nm with outer diameter greater than the 360 mm inner diameter of the rim used for the wheels of the prototype vehicle. Thereby, a two-stage machine arrangement is needed, being each machine stage rated 107.5 Nm, 1100 rpm.

Design of the prototype motor was based on the desire for high efficiency to minimize the machine cooling requirement, and the design which emerged as the most favorable of those meeting the specifications is described by the leading characteristics given in Table II. At 1100 rpm each stage of the machine develops a line-to-line peak EMF of 220 V, and the machine rating torque of 215 Nm is achieved with each stage fed by a sinusoidal waveform three-phase current having peak value of 65 A. If operated at the maximum speed with the two stages connected in series the prototype motor develops its rating torque with 93% efficiency. However, this mode of operation requires that the inverter input dc link be operated at maximum voltage of about 550-600 V, and this is found to be an unsuitable voltage level for the desire of using low-cost standard components (e.g. IGBTs rated 600 V and single electrolytic capacitors rated 450 V) for the power converter interface.

By switching the connection between the machine stages from series to parallel at half the maximum speed of the vehicle, the line-to-line EMF at the machine terminals can be kept either below or equal to 220 V, as shown in Fig. 5A. Hence, a speed-controlled dc voltage with maximum value in the range from 300 to 360 V can be used at the inverter input terminals to supply either the 100% overload or rating current against the line-to-line peak EMF developed by the machine. Fig. 5 B shows the curves of the torque and power delivered by the motor at the wheel axle over the range of speed of the prototype vehicle. As shown, switching the connection between the machine stage reduces to a half the machine torque, but this does not result in a significant drawback, as generally the vehicle is operated with speed in the range from 55 to 110 km/h if moving on a flat road, and under such a load condition the electric propulsion system still have acceptable torque capability for accelerating the vehicle.

Table II Leading characteristics of the prototype motor.

Number of poles	16
Rating speed	1100 rpm
Rating torque	215 Nm
Peak torque	430 Nm
Winding phases	3
Line-to-line peak EMF (@ 1100 rpm) (*)	220 V
Phase resistance (@ 60°C) (*)	0.13 Ω
Phase self inductance (*)	140 μH
Cooling water flow	8-12 l/min
Machine outer diameter	320 mm
Machine axial length	83 mm
Machine weight	26.8 kg

(*) Values referred to each stage of the machine.

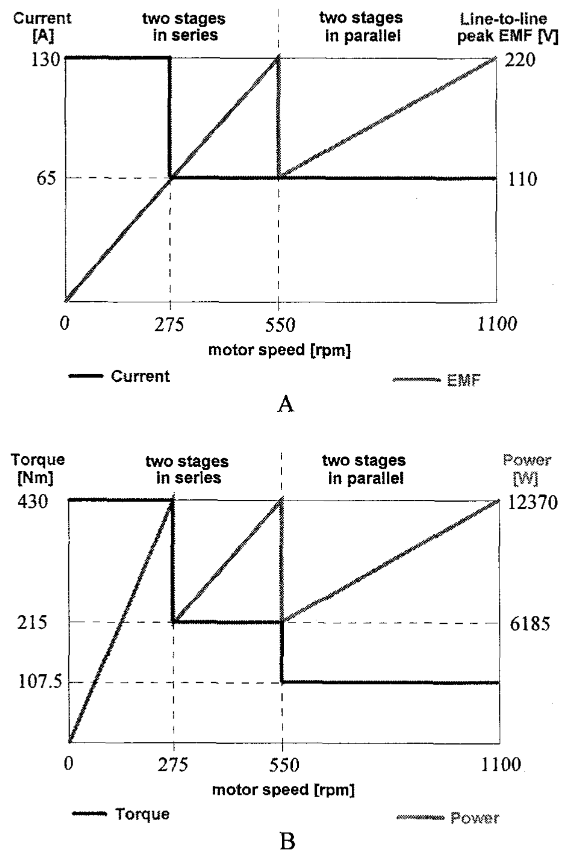

Fig. 5 Curves of operation vs. speed of the prototype motor: A, peak current and line-to-line EMF at the machine terminals; B, torque and power at the wheel axle.

Fig. 6 shows an external view of the complete axial-flux PM motor having the design characteristics given in Table II. This prototype motor has three disc rotors with surface-mounted Nd-Fe-B permanent magnets. The two external disc rotors are of mild-steel, whereas the intermediate disc rotor is of aluminium. The stator winding has 48 rhomboidal coils of rectangular copper strip. The winding coils are placed side-by-side in a toroidal fashion and then immersed in a fiberglass-reinforced epoxy resin to form a rigid body. A cooling duct of about 4 mm thickness is left between the active sides of the winding coils.

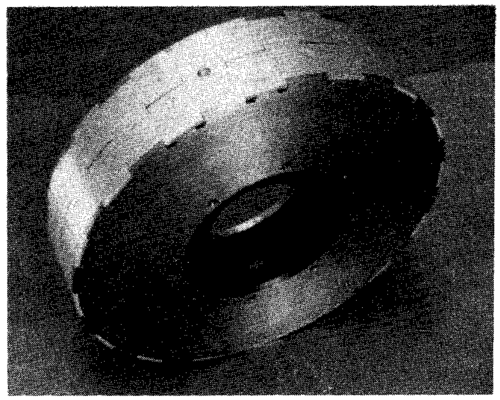

Fig. 6 View of the two-stage machine prototype.

B. Prototype of the Power Electronic Interface

Design of the power electronic interface is based on the peak voltage and current imposed by the motor operation. If assumed that a 20% current ripple is superimposed to the commanded sinusoidal current waveform at the maximum loading, from the preceding Fig. 5A it is found that the inverter bridge switches have to deal with a peak current of about 150 A. On the other hand, voltage rating of the inverter switches is determined by the maximum voltage at which the dc link is operated. By including suitable margin to take into account both voltage ripple at the inverter input terminals and transient overvoltages due to the command of a sudden braking action, voltage rating of 450 V can be assumed for the components of the power converter interface.

Rating of the buck-boost converter components relies on the assessment of the maximum peak current in the inductor determined by the converter modes of operation. As mentioned in a preceding section, the buck-boost converter is used to continuously adjust the inverter input voltage in accordance with the speed of the vehicle. Either step-down or step-up modes of operation occur depending on both the voltage required at the inverter input terminals and the battery charge level. For a given value V_b of the battery voltage, the converter output voltage V_o is determined from the expression:

$$V_o = \frac{D_{dw}}{1 - D_{up}} V_b \qquad (2)$$

where is either:

$0<D_{dw}< 1$; $D_{up}= 0$ for step-down modes of operation, or

$D_{dw}= 1$; $0<D_{up}< 1$ for the step-up modes of operation.

Since the voltage V_o required at the inverter input terminals is determined by the speed of the vehicle, values of the duty-cycles D_{dw} and D_{up} can be calculated from (2) to find out the maximum average current $I_{L(max)}$ in the inductor. Hence, for given switching frequency f_s and desired value $\Delta i\%$ of the inductor current ripple the required inductance can be calculated from the expression:

$$L = \frac{V_b\left[D_{up} + D_{dw}\left(1 - D_{dw}\right)\right]}{\Delta i\% I_{L(max)}} 100 \qquad (3)$$

and thereby the maximum peak current is calculated as:

$$I_{L(peak)} = \left(1 + \frac{\Delta i\%}{200}\right) I_{L(max)} \qquad (4)$$

Using the above described design procedure it was found that the switches of the buck-boost converter can have current rating same as the one used for the inverter switches, provided that an inductor rated 240 μH, 120 A is utilised in the dc link of the converter prototype .

Then, a prototype of the power electronic interface shown in Fig. 1 was assembled by using third-generation IGBT dual modules rated 600 V, 300 A, ferrite-core inductor rated 240 μH, 120 A, and electrolytic capacitors, each rated 2200 μF, 450 V. The IGBTs are operated at 15 kHz switching frequency. The selected IGBT modules are somewhat oversized with respect to the kVA rating actually required, but this is due to a perspective for using various types of battery storage arranged with slightly different voltage rating in the course of the road test programme of the prototype vehicle.

One significant feature of the power converter prototype is that both the IGBT modules and ferrite-core inductor are mounted on a water-cooled heat sink, which was suitably designed to reduce size and weight of the power converter. As shown in Fig. 7, the heat sink is composed by two aluminium plates, one of which has a winding-shaped duct on one of its surfaces. The two plates are to be joined together in order to form a single body with an inside cooling duct, so that the power components can be mounted on the two available surfaces, as shown in Fig. 8.

The ferrite-core inductor was constructed by using 8 double E-cores placed side by side to achieve the required cross-sectional area of the core. Table III gives characteristics of the ferrite-core inductor shown in Fig. 8. Fig. 9 shows the prototype converter during the assembling.

Table III Leading characteristics of the ferrite-core inductor.

Inductance	240 μH
Rating rms current	120 A
Rating frequency	15 kHz
Core cross-sectional area	8 x 200 mm^2
Cross-sectional area for winding	1200 mm^2
Airgap length	4 mm
Number of turns	16

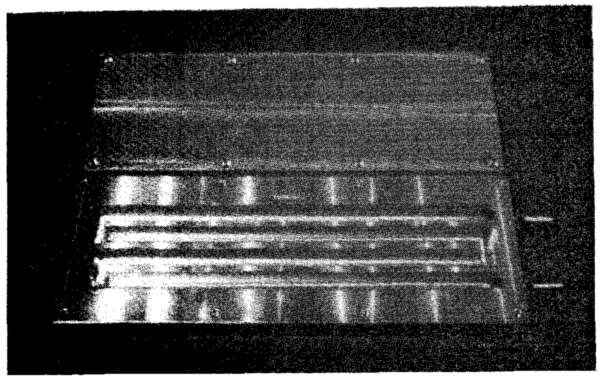

Fig. 7 The two halves composing the water-cooled heat sink with inside winding-shaped cooling duct.

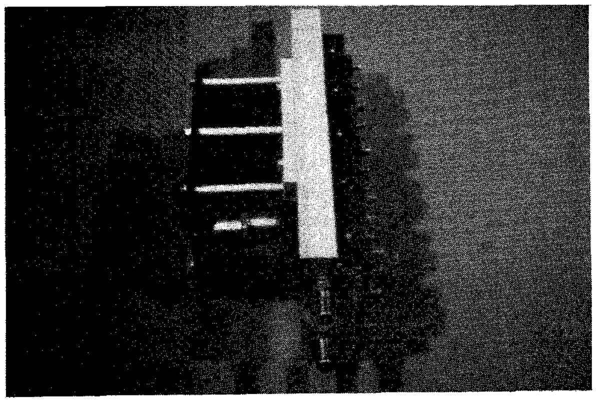

Fig. 8 IGBT power modules and ferrite-core inductor mounted on the water cooled heat sink.

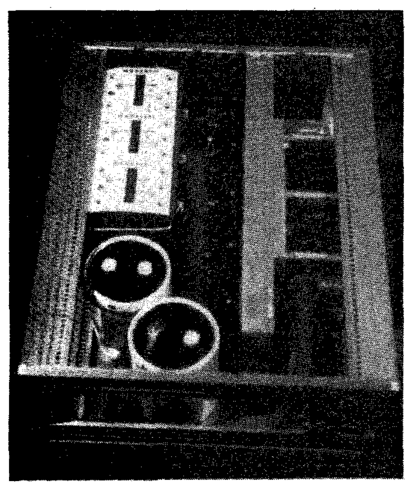

Fig. 9 The prototype converter during the assembling.

4. CONCLUSIONS

This paper has discussed design and construction of a prototype of wheel direct drive which uses an axial-flux PM motor having multi-stage structure and water-cooled air-wound stator winding. Laboratory tests of the prototype drive are being carried out, and a second identical drive is going to be constructed to complete the electric propulsion system of a novel city car for a road test programme.

ACKNOWLEDGEMENTS

This work is being developed in co-operation with the *Pininfarina Studi e Ricerche* and funded by the *CNR - Progetto Finalizzato Trasporti 2*. The authors wish to thank Mr. M. J. Marcheggiani for the assistance given in the construction of the IGBT power converter prototype.

REFERENCES

[1] F. Caricchi, F. Crescimbini, E. Fedeli, G. Noia - Design and Construction of a Wheel-Directly-Coupled Axial-Flux PM Motor Prototype for EVs - Proc. of the 1994 IEEE-IAS Annual Meeting, Denver, Colorado (USA), October 2 - 7, 1994.

[2] F. Caricchi, F. Crescimbini - Axial-Flux Permanent-Magnet Machine with Water-Cooled Ironless Stator" - Proc. of the IEEE Power Tech Conference, 1995, Stockholm, June 18-22, 1995, pp. 98-103.

[3] F. Caricchi, F. Crescimbini, Di Napoli - 20 kW Water-Cooled Prototype of a Buck-Boost Bidirectional DC-DC Converter Topology for Electric Vehicle Motor Drives - Proc. of the IEEE 10th Applied Power Electronics Conference and Exposition, Dallas, Texas (USA), March 5 - 9, 1995.